DOI: 10.1002/ejic.200800732

Halide Activation by Heme Peroxidases: Theoretical Predictions on Putative Adducts of Halides with Compound I

Radu Silaghi-Dumitrescu*[a]

Keywords: Porphyrinoids / Density functional calculations / Enzyme models / Structure–activity relationships

The first density functional theory (DFT) results on models of the putative Fe^{III}–OX and Fe^{III}–HOX (X = halogen) adducts of chloroperoxidase (CPO) and myeloperoxidase (MPO) are reported, and their stability and electronic structure assessed. The oxygen–halogen bonds are computed to be particularly weak, to the extent where ferric hypohalous acid complexes with intact oxygen–halide bonds should be difficult to observe in heme peroxidases; a 'caged' adduct, featuring a ferric species in close (but not covalent) contact with the oxidized halide, appears as a likely alternative for an observable intermediate in CPO and MPO. The presence of an axial thiolate (CPO) or imidazole (MPO) ligand in a position *trans* to the hypohalous moiety is calculated to have a distinct effect on halide activation, with relevance to the TSR (two-state reactivity) concept.

Introduction

Compound I, the peroxide-derived high-valent ferryl iron species of heme peroxidases such as chloroperoxidase (CPO) and myeloperoxidase (MPO), performs a two-electron oxidation of halides to formally generate hypohalous acids, HOX, which can either be released or used for halogenation reactions.[1–7] Most peroxidases oxidize iodide, some oxidize bromide, and very few (of which MPO and CPO are classical examples) are known to oxidize chloride. It is generally accepted that halide oxidation occurs at or very near the heme; the crystal structure of a bromide adduct of MPO shows that the bromide is bound very close to the open sixth coordination position and is just 5 Å from the heme iron.[1] With the use of UV/Vis spectroscopy, intermediates arising from the reaction of Compound I with chloride and also those proposed to form Fe^{III} adducts with HOCl and OCl^- were detected for model compounds as well for CPO (always with a thiolate axial ligand at the heme).[2,8] However, the structure of these intermediates has not been explored/confirmed with other methods, nor have such species been detected with other peroxidases. Earlier data on other histidine-ligated peroxidases on putative hypochlorite adducts ('Compound X', 'Compound XI', Compound 'XII') were later deemed to be artefactual.[6]

Figure 1 illustrates the proposed catalytic pathways for hemoproteins that react with H_2O_2/halide systems. It is generally accepted that Compound I, formally Fe^V but better described as a ferryl (Fe^{IV}=O) and a porphyrin cation radical, is the species that reacts with the halide. In this paper, density functional theory (DFT) results on models of the putative Fe^{III}–OX and Fe^{III}–HOX adducts of CPO and MPO are reported, and their stability and electronic structure assessed. The oxygenhalogen bonds are computed to be particularly weak, to the extent where ferric hypohalous acid complexes with intact oxygen–halide bonds should be difficult to observe in heme peroxidases; a 'caged' adduct, featuring a ferric species in close (but not covalent) contact with the oxidized halide, appears as a likely alternative for

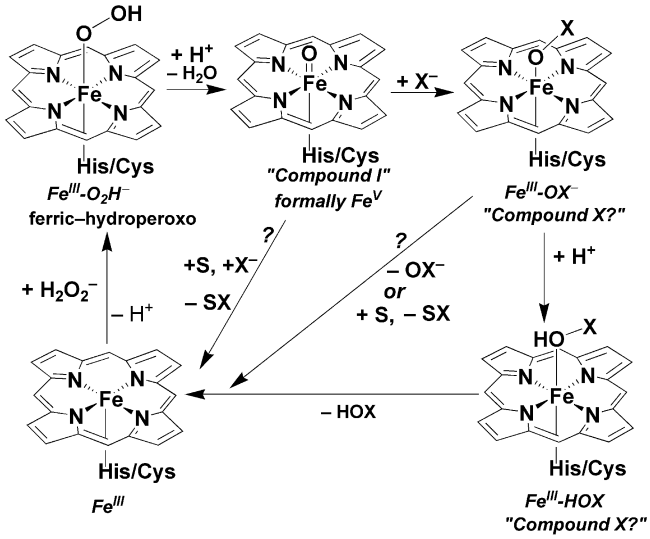

Figure 1. Reactivity of myeloperoxidase-type (histidine-ligated) and chloroperoxidase-type (thiolate-ligated) heme peroxidases towards the peroxide/halide system. 'S' denotes an organic substrate; 'X' denotes a halide (typically chloride).

[a] Department of Chemistry, Babeş-Bolyai University, Cluj-Napoca 400028, Romania
E-mail: rsilaghi@chem.ubbcluj.ro

Supporting information for this article is available on the WWW under http://www.eurjic.org or from the author.

an observable intermediate in CPO and MPO. The presence of an axial thiolate (CPO) or imidazole (MPO) ligand in a position *trans* to the hypohalous moiety is calculated to have a distinct effect on halide activation.

Results and Discussion

Structure and Reactivity of Ferric–Hypochlorite Adducts

Table 1 lists computed energies, key geometrical parameters, and relevant elements of the Mulliken population analyses of OCl^- and HOCl adducts of imidazole- and methyl thiolate ligated ferric hemes as models for histidine- and cysteine-ligated enzymes, respectively (Figure 1). The OCl^- adducts feature Fe–O bonds ranging from 1.77 to 1.94 Å; these values are in the same range as those previously reported at the same level of theory for ferric–hydroperoxo adducts (1.80–1.89 Å) and are consistent with a ferric–hypochlorite description. The Fe–O bonds computed for the imidazole-ligated models are shorter than in the corresponding thiolate models, in line with the previously observed *trans* effect of the thiolate, which destabilizes the *trans* ligand by Fe–S orbital mixing.[9–11] The O–Cl bond lengths correlate inversely with the Fe–O bond lengths (in a manner similar to that observed for numerous related diatomic ligands, such as dioxygen or peroxide[11–13]), and are just barely longer than those calculated at the same level of theory for an isolated HOCl molecule (1.74–1.80 Å in the hypochlorite models relative to 1.73 Å in free HOCl); these findings support the concept that a 'Compound X' species is a feasible detectable intermediate in enzymes and/or model compounds.

The proton affinities of the OCl^- adducts are 327 and 244 kcal/mol for the thiolate- and imidazole-ligated models, respectively; these values may be compared to the proton affinities of species with similar sizes, chemical compositions, and overall charges, for which the experimental pK_a values are also known;[12,14,15] for both thiolate- and imidazole-ligated models, this comparison suggests relatively acidic pK_a values, with the deprotonated state predominating at neutral pH. The stability of the deprotonated Fe–O–Cl moiety was probed, as seen in Figure 2 where the energy required for the lengthening of the O–Cl bond is shown. This cost is extremely low (≈10 kcal/mol), which, on the basis of computations at the same level of theory[12], indicates that the heme hypochlorite adducts are as stable as the elusive Compound I of cytochromes P450. One important conclusion is that protonation is not required for extremely facile O–Cl bond cleavage nor is this protonation likely to occur in the neutral pH range. Conversely, Figure 2 may also be interpreted as showing an extremely small activation barrier for halide binding/oxidation by the Compound I species. It is particularly interesting to note the topology of the system at the 3.0-Å O–Cl distance (right-most data point in Figure 2): the Fe–Cl distance is now 4.3 Å, and the Cl–heme distance is 3.8 Å. Remarkably, Figure 3 shows that these two parameters are essentially identical to those seen for the resting ferric state of a haloperoxidase with a halide bound at the active site.

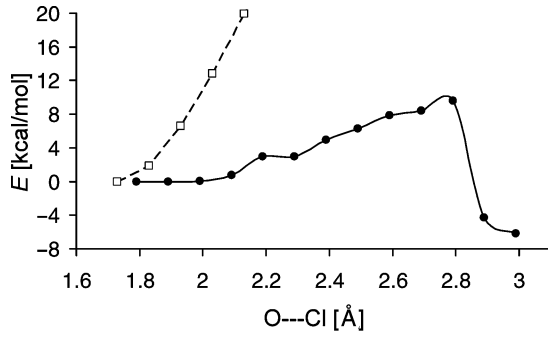

Figure 2. Potential energy surface for O–Cl bond elongation (filled circles) in the S = 1/2 thiolate-ligated Fe–O–Cl model (similar results were obtained for the imidazole-based model, not shown). The open squares represent points on the equivalent potential surface in an isolated HOCl molecule, as a reference.

Table 1 shows that the protonated versions of the thiolate models, Fe–O(H)–Cl, feature particularly elongated O–Cl bonds (2.12 and 2.37 Å for the S = 1/2 and S = 3/2 states, respectively), while the S = 1/2 imidazole model shows an 1.98-Å bond; all these bonds are distinctly longer than the 1.73-Å bond computed for free HOCl at the same level of theory. It is thus seen that binding to iron dramatically weakens the O–Cl bond, to the extent where, in the thiolate models especially, it is essentially broken. On the other hand, the S = 3/2 imidazole-ligated model is somewhat different, with an extremely weak (2.46 Å) Fe–O interaction and an HOCl ligand that is essentially free of the iron (the

Table 1. Relative energies of [kcal/mol], geometries of [Å], charges on, and spin densities (the latter shown in square brackets) on the OCl^- and HOCl adducts of unsubstituted ferric hemes with methyl thiolate ('S') or imidazole ('N') axial ligands. 'P' and 'ax' denote summed partial atomic charges and spin densities on the porphyrin ring and on the imidazole/methyl thiolate ligand, respectively. Relative energies are referenced to the most stable state in each of the two series of models (thiolate, imidazole), respectively.

Model	Relative energies	Fe–O	O–X	Fe–S/N	Fe	O	Cl	P	ax
S = 1/2 S/Fe^{III}/OCl^-	0.0	1.86	1.79	2.30	0.45 [0.71]	–0.44 [0.18]	–0.01 [0.01]	–0.84 [–0.09]	–0.16 [0.19]
S = 3/2 S/Fe^{III}/OCl^-	17.8	1.92	1.74	2.35	0.49 [1.74]	–0.44 [0.36]	0.03 [0.15]	–0.84 [0.39]	–0.12 [0.36]
S = 1/2 N/Fe^{III}/OCl^-	0.0	1.77	1.80	2.09	0.56 [0.73]	–0.37 [0.27]	0.06 [0.03]	–0.54 [–0.02]	0.29 [–0.01]
S = 3/2 N/Fe^{III}/OCl^-	13.0	1.94	1.70	2.39	0.68 [2.34]	–0.48 [0.42]	0.13 [0.16]	–0.50 [0.02]	0.17 [0.06]
S = 1/2 S/Fe^{III}/HOCl	–326.9	1.91	2.12	2.21	0.41 [0.86]	–0.39 [–0.05]	–0.17 [–0.15]	–0.34 [–0.02]	0.14 [0.36]
S = 3/2 S/Fe^{III}/HOCl	–321.6	1.90	2.37	2.24	0.44 [1.34]	–0.41 [0.41]	–0.27 [0.65]	–0.21 [0.16]	0.14 [0.44]
S = 1/2 N/Fe^{III}/HOCl	–243.9	1.89	1.98	1.99	0.56 [0.87]	–0.39 [–0.01]	0.01 [–0.10]	0.03 [0.26]	0.41 [–0.02]
S = 3/2 N/Fe^{III}/HOCl	–242.7	2.46	1.75	2.18	0.71 [2.56]	–0.47 [0.03]	0.17 [0.02]	–0.08 [0.38]	0.31 [0.11]

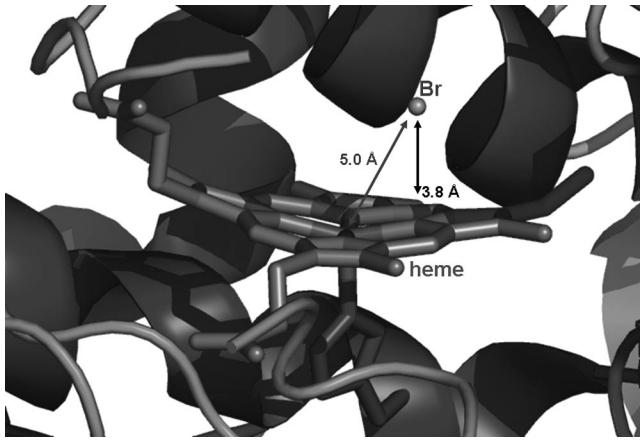

Figure 3. Iron–halide and halide–heme distance in the crystal structure of the ferric–bromide adduct of myeloperoxidase (pdb code 1D2V). Distances from the bromide to the iron and to the closest atom of the heme are shown.

HO–Cl distance of 1.75 Å is almost identical to that computed for free HOCl, see above). This fact is notable, as for the imidazole-ligated models, the $S = 3/2$ state is most likely preferred over the $S = 1/2$ state (they are calculated to be degenerate, but our BP86 functional is known to overestimate the stability of lower-spin states). By contrast, in the thiolate-ligated model, there is a stronger preference for the $S = 1/2$ state, and the $S = 3/2$ still favors an unusually elongated O–Cl distance (2.4 Å) – essentially a broken bond. In this latter case, the spin densities shown in Table 1 and Figure 4 are also indicative of a Cl atom character for the chlorine (0.65 spins on Cl), which implies an Fe^{IV} character. A similar Fe^{IV} character is (less) noticeable in the $S = 1/2$ thiolate- and imidazole-ligated Fe–O(H)–Cl models, with an antiferromagnetic coupling between Cl and the Fe–OH moiety. By contrast, the nonprotonated adducts feature spin densities and partial atomic charges well consistent with Fe^{III}, with negligible Fe^{IV} contribution.

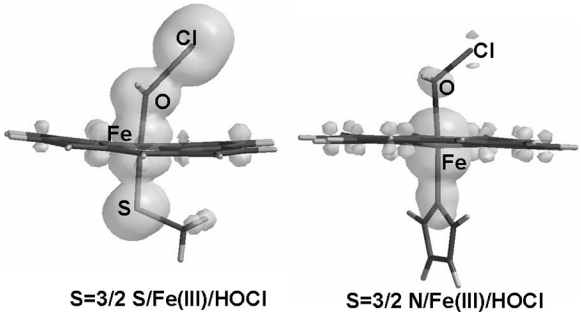

Figure 4. Spin densities computed for the $S = 3/2$ thiolate- and imidazole-ligated Fe^{III}–HOCl models (see Figure 1 and Table 1).

The conclusion of this section is therefore that the oxygen–chloride bonds are computed to be particularly weak, to the extent where ferric hypohalous acid complexes with intact oxygen–halide bonds should be difficult to observe in heme peroxidases; a 'caged' adduct, featuring a ferric species in close (but not covalent) contact with the oxidized halide, appears as a likely alternative for an observable intermediate in CPO and MPO.

Role of the Axial Ligand in Halide-Activating Peroxidases

The notable difference in reactivity between the thiolate- and imidazole-ligated Fe–O(H)–Cl adducts (the imidazole model shows a stronger preference for the $S = 3/2$ state and for Fe–O bond cleavage and the thiolate model favors the $S = 1/2$ state and O–Cl bond cleavage) is yet another manifestation of the 'two-state reactivity' theory introduced by Shaik and co-workers for high-valent heme systems.[16,17] Our findings in this respect are in excellent agreement with experimental results: the physiological function of the thiolate-ligated CPO is to precisely cleave the O–Cl bond and insert the Cl into an organic substrate, while that of the histidine-ligated MPO is part of a nonspecific immune response wherein it mainly liberates HOCl.

Role of Heme Modifications in Halide Activation

The above data suggest that there is little need for the heme periphery in order to achieve halide activation. Histidine-bound haloperoxidases do tend to show covalent modifications at the heme edge, and it is known that at least some of these modifications dramatically increase the haloperoxidase activity. However, as pointed out by experimentalists,[18–21] these covalent modifications do not abolish peroxidase activity in general and are rather associated with increased heme rigidity and better halide binding. In view of our results reported above, we also support the notion that there is no intrinsic electronic-structure rationale for heme edge modification in haloperoxidases and that these modifications are part of a mechanism to create a halide binding site near the heme – binding that apparently also requires some degree of pocket rigidity (possibly connected to the slight endergonicity of halide binding to Compound I, Figure 2). The role of heme rigidity/mobility is not unique to haloperoxidases among hemoproteins. In heme oxygenases, an increased degree of heme mobility has at times been invoked as required for heme activation by the reactive ferric–peroxo intermediate;[22,23] by contrast, computational data[9,24,25] suggests that no particular 'priming' by the protein matrix is required and that simple models lacking the polypeptide moiety can just as well perform heme oxygenase chemistry, but that it is indeed essential for the protein to *allow* heme deformation during the course of the reaction. These observations on the role of the protein matrices in haloperoxidases and heme oxygenases are of course in line with the concept that the role of the polypeptide moieties in proteins is often to *selectively allow certain reactions, as opposed to creating new chemistry.*

Conclusions

Density functional theory (DFT) results on models of the putative Fe^{III}–OX and Fe^{III}–HOX adducts of CPO and

MPO are reported here, and their stability and electronic structure assessed. The oxygen–halogen bonds are computed to be particularly weak, to the extent where ferric hypohalous acid complexes with intact oxygen–halide bonds should be difficult to observe in heme peroxidases; a 'caged' adduct, featuring a ferric species in close (but not covalent) contact with the oxidized halide, appears as a likely alternative for an observable intermediate in CPO and MPO. The presence of an axial thiolate (CPO) or imidazole (MPO) ligand in a position *trans* to the hypohalous moiety is calculated to have a distinct effect on halide activation.

Experimental Section

Density functional calculations on unsubstituted iron porphyrin adducts listed in Table 1 and illustrated in Figure 1 were performed by employing imidazole- and methyl thiolate ligands to mimic the protein-derived histidine and cysteinate ligands, respectively. Alternatives to the Fe–O–Cl adducts, with Fe–Cl–O topology, have not been considered in line of previously available data on related ferric–hydroperoxo adducts Fe–O(H)–O (OH isolobal to Cl), where the Fe–OH bond was seen to be too weak to allow O–OH bond activation and the energy of the isomers was higher than that of the canonical Fe–O–OH forms.[10,12] Likewise, HOCl carries its proton on the oxygen atom and not on the chlorine atom. An S_N2 reaction, involving the attack of the chloride on the iron-bound oxygen in Fe^{III}–O–OH was not investigated, in light of previous data indicating that the cleavage of the O–O bond is already extremely facile, even in the absence of the halide.[9] Geometries were optimized for each spin state without any geometrical constraints, with the BP86 functional, which uses the gradient-corrected exchange functional proposed by Becke (1988),[26] the correlation functional by Perdew (1986),[27] and the DN** numerical basis set (comparable in size to 6-31G**), as implemented in Spartan.[28] For the SCF calculations, a fine grid was used, and the convergence criteria were set to 10^{-6} (for the root-mean-square of the electron density) and 10^{-8} (energy). For geometry optimization, convergence criteria were set to 0.001 au (maximum gradient criterion) and 0.0003 (maximum displacement criterion). Charges and spin densities were derived from Mulliken population analyses after DFT geometry optimization. Proton affinities were obtained in vacuo, but the trends are readily maintained in solvents.[12,14,15]

Supporting Information (see footnote on the first page of this article): Coordinates for the optimized models.

Acknowledgments

Funding from the Romanian Ministry of Education and Research (grant CEEX-ET-98) and the Romanian Academy (grant 63/28.08.2007) is gratefully acknowledged.

[1] T. J. Fiedler, C. A. Davey, R. E. Fenna, *J. Biol. Chem.* **2000**, *275*, 11964–11971.
[2] W. D. Woggon, *Acc. Chem. Res.* **2005**, *38*, 127–136.
[3] L. Huang, G. Wojciechowski, P. R. Ortiz de Montellano, *J. Am. Chem. Soc.* **2005**, *127*, 5345–5353.
[4] J. Arnhold, P. Furtmuller, C. Obinger, *Redox Rep.* **2003**, *8*, 179–186.
[5] R. Silaghi-Dumitrescu, *Horseradish Peroxidase – A Versatile Catalyst*, Research Signpost, India, **2006**.
[6] J. Everse, K. Everse, B. M. Grisham, *Peroxidases in Chemistry and Biology*, CRC Press, Boca Raton, **1991**.
[7] R. Floris, R. Wever, *Eur. J. Biochem.* **1992**, *207*, 697–702.
[8] H. B. Dunford, A. M. Lambeir, M. A. Kashem, M. Pickard, *Arch. Biochem. Biophys.* **1987**, *252*, 292–302.
[9] R. Silaghi-Dumitrescu, I. Silaghi-Dumitrescu, *Chemtracts Inorg. Chem.* **2005**, *18*, 595–619.
[10] R. Silaghi-Dumitrescu, I. Silaghi-Dumitrescu, E. D. Coulter, D. M. Kurtz Jr, *Inorg. Chem.* **2003**, *42*, 446–456.
[11] R. Silaghi-Dumitrescu, I. Silaghi-Dumitrescu, *Rev. Roum. Chim. 3* **2004**, *4*, 257–268.
[12] R. Silaghi-Dumitrescu, C. E. Cooper, *Dalton Trans.* **2005**, *403*, 3477–3482.
[13] P. Rydberg, E. Sigfridsson, U. Ryde, *J. Biol. Inorg. Chem.* **2004**, *9*, 203–223.
[14] R. Silaghi-Dumitrescu, B. J. Reeder, P. Nicholls, C. E. Cooper, M. T. Wilson, *Biochem. J.* **2007**, *403*, 391–5.
[15] R. Silaghi-Dumitrescu, *J. Biol. Inorg. Chem.* **2004**, *9*, 471–476.
[16] S. Shaik, S. P. de Visser, F. Ogliaro, H. Schwarz, I. Schröder, *Curr. Opin. Chem. Biol.* **2002**, *6*, 556–567.
[17] S. Shaik, D. Kumar, S. P. de Visser, A. Altun, W. Thiel, *Chem. Rev.* **2005**, *105*, 2279–2328.
[18] M. Zederbauer, P. G. Furtmuller, S. Brogioni, C. Jakopitsch, G. Smulevich, C. Obinger, *Nat. Prod. Rep.* **2007**, *24*, 571–584.
[19] M. Zederbauer, W. Jantschko, K. Neugschwandtner, C. Jakopitsch, N. Moguilevsky, C. Obinger, P. G. Furtmuller, *Biochemistry* **2005**, *44*, 6482–6491.
[20] M. Zederbauer, P. G. Furtmuller, B. Ganster, N. Moguilevsky, C. Obinger, *Biochem. Biophys. Res. Commun.* **2007**, *356*, 450–456.
[21] M. Zederbauer, P. G. Furtmuller, M. Bellei, J. Stampler, C. Jakopitsch, G. Battistuzzi, N. Moguilevsky, C. Obinger, *J. Biol. Chem.* **2007**, *282*, 17041–17052.
[22] J. C. Rodriguez, Y. Zeng, A. Wilks, M. Rivera, *J. Am. Chem. Soc.* **2007**, *129*, 11730–11742.
[23] M. Rivera, Y. Zeng, *J. Inorg. Biochem.* **2005**, *99*, 337–354.
[24] R. Silaghi-Dumitrescu, *Studia Univ. Babeş-Bolyai, Chemia* **2007**, *52*, 47–54.
[25] P. K. Sharma, R. Kevorkiants, S. P. de Visser, D. Kumar, S. Shaik, *Angew. Chem. Int. Ed.* **2004**, *43*, 1129–1132.
[26] A. D. Becke, *Phys. Rev.* **1988**, 3098–3100.
[27] J. P. Perdew, *Phys. Rev. B* **1986**, *33*, 8822–8824.
[28] *Spartan 5.0*, Wavefunction, Inc., Irvine, CA, U.S.A.

Received: July 24, 2008
Published Online: October 23, 2008

